Power dependence of supercontinuum noise in uniform and tapered PCFs

Møller, Uffe; Sørensen, Simon Toft; Jakobsen, C.; Johansen, J.; Moselund, Peter M.; Thomsen, C. L.; Bang, Ole

Published in:
Optics Express

Link to article, DOI:
10.1364/OE.20.002851

Publication date:
2012

Document Version
Publisher's PDF, also known as Version of record

Power dependence of supercontinuum noise in uniform and tapered PCFs

U. Møller,[1,*] **S. T. Sørensen,**[1] **C. Jakobsen,**[2] **J. Johansen,**[2]
P. M. Moselund,[2] **C. L. Thomsen,**[2] **and O. Bang**[1,2]

[1]*DTU Fotonik, Technical University of Denmark, DK-2800 Kgs. Lyngby, Denmark*
[2]*NKT Photonics A/S, Blokken 84, DK-3400 Birkerød, Denmark*
[*]*ufmo@fotonik.dtu.dk*

Abstract: We experimentally investigate the noise properties of picosecond supercontinuum spectra generated at different power levels in uniform and tapered photonic crystal fibers. We show that the noise at the spectral edges of the generated supercontinuum is at a constant level independent on the pump power in both tapered and uniform fibers. At high input power the spectral bandwidth is limited by the infrared loss edge, this however has no effect on the noise properties.

OCIS codes: (060.4370) Nonlinear optics, fibers; (060.5295) Photonic crystal fibers; (320.6629) Supercontinuum generation.

References and links

1. J. M. Dudley and J. R. Taylor, "Ten years of nonlinear optics in photonic crystal fibre," Nat. Photonics **3**, 85–90 (2009).
2. N. Savage, "Supercontinuum sources," Nat. Photonics **3**, 114–115 (2009).
3. W. Drexler, "Ultrahigh-resolution optical coherence tomography," J. Biomed. Opt. **9**, 47–74 (2004).
4. D. Wildanger, E. Rittweger, L. Kastrup, and S. W. Hell, "STED microscopy with a supercontinuum laser source," Opt. Express **16**, 9614–9621 (2008).
5. N. R. Newbury and W. C. Swann, "Low-noise fiber-laser frequency combs (Invited)," J. Opt. Soc. Am. B **24**, 1756–1770 (2007).
6. J. M. Dudley, G. Genty, and B. J. Eggleton, "Harnessing and control of optical rogue waves in supercontinuum generation." Opt. Express **16**, 3644–3651 (2008).
7. G. Genty, J. M. Dudley, and B. J. Eggleton, "Modulation control and spectral shaping of optical fiber supercontinuum generation in the picosecond regime," Appl. Phys. B **94**, 187–194 (2008).
8. D. R. Solli, C. Ropers, and B. Jalali, "Active control of rogue waves for stimulated supercontinuum generation," Phys. Rev. Lett. **101**, 18–21 (2008).
9. K. K. Y. Cheung, C. Zhang, Y. Zhou, K. K. Y. Wong, and K. K. Tsia, "Manipulating supercontinuum generation by minute continuous wave," Opt. Lett. **36**, 160–162 (2011).
10. Q. Li, F. Li, K. K. Y. Wong, A. Pak, T. Lau, and K. K. Tsia, "Investigating the influence of a weak continuous-wave-trigger on picosecond supercontinuum generation," Opt. Express **19**, 377–381 (2011).
11. P. M. Moselund, M. H. Frosz, C. L. Thomsen, and O. Bang, "Back-seeding of higher order gain processes in picosecond supercontinuum generation," Opt. Express **16**, 11954–11968 (2008).
12. P. Falk, M. Frosz, and O. Bang, "Supercontinuum generation in a photonic crystal fiber with two zero-dispersion wavelengths tapered to normal dispersion at all wavelengths," Opt. Express **13**, 7535–7540 (2005).
13. P. M. Moselund, "Long-pulse supercontinuum light sources," PhD thesis (Technical University of Denmark, Denmark, 2009).
14. A. Kudlinski, B. Barviau, A. Leray, C. Spriet, L. Héliot, and A. Mussot, "Control of pulse-to-pulse fluctuations in visible supercontinuum," Opt. Express **18**, 27445–27454 (2010).
15. D. Buccoliero, H. Steffensen, H. Ebendorff-Heidepriem, T. M. Monro, and O. Bang, "Midinfrared optical rogue waves in soft glass photonic crystal fiber," Opt. Express **19**, 17973–17978 (2011).
16. J. M. Dudley, G. Genty, and S. Coen, "Supercontinuum generation in photonic crystal fiber," Rev. Mod. Phys. **78**, 1135–1184 (2006).

#159492 - $15.00 USD Received 7 Dec 2011; revised 3 Jan 2012; accepted 15 Jan 2012; published 23 Jan 2012

17. K. L. Corwin, N. R. Newbury, J. M. Dudley, S. Coen, S. A. Diddams, K. Weber, and R. S. Windeler, "Fundamental noise limitations to supercontinuum generation in microstructure fiber," Phys. Rev. Lett. **90**, 113904 (2003).
18. A. Hartung, A. M. Heidt, and H. Bartelt, "Design of all-normal dispersion microstructured optical fibers for pulse-preserving supercontinuum generation," Opt. Express **19**, 7742–7749 (2011).
19. O. Vanvincq, B. Barviau, A. Mussot, G. Bouwmans, Y. Quiquempois, and A. Kudlinski, "Significant reduction of power fluctuations at the long-wavelength edge of a supercontinuum generated in solid-core photonic bandgap fibers," Opt. Express **18**, 24352–24360 (2010).
20. C. Lafargue, J. Bolger, G. Genty, F. Dias, J. M. Dudley, and B. J. Eggleton, "Direct detection of optical rogue wave energy statistics in supercontinuum generation," Electron. Lett. **45**, 217–219 (2009).
21. D. R. Solli, C. Ropers, P. Koonath, and B. Jalali, "Optical rogue waves," Nature **450**, 1054–1057 (2007).
22. D. Derickson, ed., *Fiber Optic Test and Measurement* (Prentice Hall, 1998).
23. P. Beaud, W. Hodel, B. Zysset, and H. Weber, "Ultrashort pulse propagation, pulse breakup, and fundamental soliton formation in a single-mode optical fiber," IEEE J. Quantum Electron. **23**, 1938–1946 (1987).
24. F. Biancalana, D. V. Skryabin, and P. S. Russell, "Four-wave mixing instabilities in photonic-crystal and tapered fibers," Phys. Rev. E **68**, 046603 (2003).
25. A. V. Gorbach and D. V. Skryabin, "Light trapping in gravity-like potentials and expansion of supercontinuum spectra in photonic-crystal fibres," Nat. Photonics **1**, 653–657 (2007).
26. J. M. Stone and J. C. Knight, "Visibly 'white' light generation in uniform photonic crystal fiber using a microchip laser," Opt. Express **16**, 2670–2675 (2008).
27. J. C. Travers, "Blue extension of optical fibre supercontinuum generation," J. Opt. **12**, 113001 (2010).
28. S. Pricking and H. Giessen, "Tailoring the soliton and supercontinuum dynamics by engineering the profile of tapered fibers," Opt. Express **18**, 20151–20163 (2010).
29. S. T. Sørensen, A. Judge, C. L. Thomsen, and O. Bang, "Optimum fiber tapers for increasing the power in the blue edge of a supercontinuum-group-acceleration matching," Opt. Lett. **36**, 816–818 (2011).
30. N. R. Newbury, B. R. Washburn, K. L. Corwin, and R. S. Windeler, "Noise amplification during supercontinuum generation in microstructure fiber," Opt. Lett. **28**, 944–946 (2003).

1. Introduction

Supercontinuum generation (SCG) in photonic crystal fibers (PCFs) has drawn a lot of attention during the last decade [1]. The emergence of commercial fiber-based, long-pulsed supercontinuum (SC) sources has matured the technology [2], and the unique properties of SC light sources have made them ideal tools for a number of applications, including optical coherence tomography [3], fluorescence microscopy [4], and frequency combs [5]. However, SCG in commercial SC sources is initiated by modulation instability (MI) and thus, the SC is characterized by low coherence and high shot-to-shot fluctuations at the spectral edges. Several methods have been proposed to modify the spectrum and reduce the noise, including seeding by modulation of the input pulse [6, 7], seeding with minute pulsed and cw light [8–10], and back seeding [11]. Another approach to reduce the noise at a fixed wavelength has been to taper the PCF [12–14]. The influence of the material loss edge of soft glass PCFs has also been studied in the mid-IR [15].

Short-pulsed (femtosecond) SC is dominated by soliton fission processes and is fundamentally different from MI-initiated SCG and thus has different noise properties [6, 16, 17]. However, the higher complexity and lack of high average power makes these sources less attractive. Pumping in the normal dispersion regime will also drastically change the SC properties [18].

In this paper, we compare the noise properties of long-pulsed SC generated in a tapered and a uniform PCF, at different power levels. We investigate the full spectral region of 400-2400 nm. Recently, similar work has been done by Kudlinski *et al.* where they measured the shot-to-shot variations from a uniform and a tapered fiber for one fixed power level. They defined a noise measure given by the ratio $\sigma = 100 \cdot (V_{max} - V_{min})/(V_{max} + V_{min})$, where V_{max} and V_{min} are the maximum and minimum photodiode signal amplitudes, respectively, measured for at least 10 out of 10,000 recorded pulses, and showed that the noise was reduced in the tapered fiber when observing a fixed wavelength near the blue edge [14]. In this work we measure the relative intensity noise (RIN) in the whole parameter space of input power and wavelength, including the region of the silica material loss edge above 2 μm. RIN is a standard

#159492 - $15.00 USD Received 7 Dec 2011; revised 3 Jan 2012; accepted 15 Jan 2012; published 23 Jan 2012

measure for describing power fluctuations of lasers. Another article of Vanvincq *et al.* describes a significant reduction of power fluctuations at the long-wavelength edge of a SC generated in solid-core photonic bandgap (PBG) fibers [19]. There are three main reasons why this work is distinguished from the work of Vanvincq *et al.*. Firstly, the PBG fibers are less attractive from an application point of view, since the spectral bandwidth of SC generated in PBGs will be limited and thus not utilize the full potential of silica. Secondly, there is a fundamental difference of the guiding mechanisms and the soliton dynamics in PBG fibers compared to solid core PCFs. When a soliton is approaching the bandgap edge in a PBG fiber it will experience an asymptotic change of the group velocity dispersion (GVD). This change will cause the soliton to broaden in time and decrease in peak power adiabatically. It will never cross the bandgap edge due to the temporal broadening (and thereby reduction in redshift) arising from the increasing dispersion. Near the loss edge in a PCF the soliton will experience more or less the same GVD when redshifting, and the soliton energy will drop because of the gradually increasing material loss. However, it is still possible for the solitons to propagate into the loss region, with high-power solitons penetrating furthest. Since the soliton dynamics is different it is not obvious that the noise properties are the same for the two fibers. Thirdly, Vanvincq *et al.* investigated the noise properties at one power level where the spectrum was not limited by the material loss edge.

2. Experimental setup

For the experiments we used an ytterbium (Yb) fiber laser (NKT Photonics A/S) which delivers 10 ps pulses at 1064 nm at a repetition rate of 80 MHz. The laser delivery fiber was spliced to the PCFs to minimize coupling losses and instabilities. The PCF input power was 10 W, corresponding to a pulse energy of 125 nJ and a peak power of 11.7 kW when assuming Gaussian shaped pulses. The generated SC output was collimated and the spectra were measured with optical spectrum analyzers. The collimated SC output was guided through narrow-band pass filters (NBPs) of 10-30 nm full width at half maximum (450-1600 nm filters from Thorlabs and 1810-2310 nm from Multi-IR Optoelectronics Co., Ltd) and onto a photoreceiver (PR) (Newfocus 125 MHz Si and InGaAs photoreceivers for measurements in the 450-1000 and 1000-1600 nm range, respectively, and a Redwave Labs 100 MHz extended InGaAs photoreceiver for measurements in the 1600-2400 nm range). The photoreceiver was connected to an electrical spectrum analyzer (ESA) (sweeping for 30 s with a bandwidth of 10 kHz) and a voltmeter (V) to characterize the DC and AC voltage, respectively. A sketch of the experimental setup is shown in Fig. 1(a).

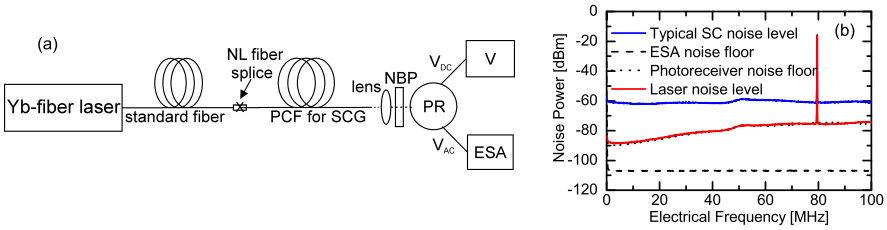

Fig. 1. (a) Experimental setup, see detailed description in text. (b) Noise power as a function of electrical frequency for a typical SC (blue line, 6.4 W input power at 1200 nm) and laser at 1064 nm (red line), respectively, and the noise floor for the electrical spectrum analyzer (dashed line) and the photoreceiver (dotted line), respectively.

Since the energy of the spectrally filtered pulses is proportional to their peak power, this measurement technique is adequate for measuring the shot-to-shot fluctuations [20, 21]. The RIN of the filtered wavelengths, i.e. the time series of power through the filters, were calculated

#159492 - $15.00 USD Received 7 Dec 2011; revised 3 Jan 2012; accepted 15 Jan 2012; published 23 Jan 2012

in the electrical frequency range of 20 kHz to 80 MHz. A full noise power spectrum is shown in Fig. 1(b). The dashed black line shows the noise floor of the electrical spectrum analyzer (ESA). The dotted line indicates the photoreceiver noise floor while the red line indicates the laser noise level. Note that the laser noise level and the photoreceiver noise floor in fact are indistinguishable, except at the carrier frequency of 80 MHz and thus it is not sensitive enough to resolve the real laser noise level. The blue line shows the noise power of a typical SC, which easily can be detected by the photoreceiver. When the DC photocurrent is simultaneously monitored, the noise properties of the SC can be quantified in terms of RIN as a function of wavelength and input power [22].

3. Results and discussion

3.1. Spectral characterization

A commercially available PCF (SC-5.0-1040, NKT Photonics A/S) with a total length of 10 m and a 4 m, asymmetric taper was fabricated directly on the draw-tower. This tapered fiber was compared to a uniform fiber of the same length. The output spectra for an input power of 10 W are depicted in Fig. 2(a) and profile of the tapered fiber is shown in the inset of Fig. 2(a). The fiber pitch was calculated from the continuous monitoring of the fiber diameter assuming that they are proportional. This was confirmed by several microscope images of the fiber cross section throughout the fiber. The tapered fiber is pumped from the fiber-end which gives most power in the blue edge according to the principle of group acceleration mismatch (GAM) [29]. The blue edge of the SC generated in the uniform fiber at a level of -10 dBm/nm is measured to

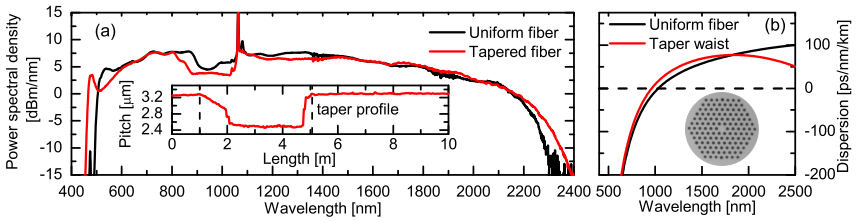

Fig. 2. (a) Spectra from a 10 m uniform PCF (black) and a 10 m PCF with a 4 m taper (red). Inset in (a): profile of the tapered fiber. (b) Calculated dispersion of the uniform fiber (black) and the taper waist (red). Inset in (b): microscope image of the fiber cross section.

be at 493 nm while it is 35 nm lower at 458 nm for the SC generated in the tapered fiber. The red edges of the SCs generated in the fibers are both limited by the IR material loss and at a -10 dBm/nm level they are measured to be at 2297 nm and 2342 nm for the uniform and tapered fiber, respectively. Figure 2(b) shows the calculated dispersion of the uniform fiber and at the taper waist, and the inset shows the cross sectional structure of the fiber.

The spectral edges of the SC are comprised by solitons and group-velocity (GV) matched dispersive waves [23–26]. The maximum spectral width and the position of the blue edge can hence be estimated from calculated GV curves. By tapering the fiber one can blueshift the blue edge [27–29]. For fibers with only one zero-dispersion wavelength (ZDW), such as the one we have here (see Fig. 2(b)), tapering will lead to an increased nonlinearity and thus in general to an increased redshift of solitons compared to a uniform fiber. For a given taper length and degree of tapering, the longer the downtapering the more power is in the dispersive waves trapped by the solitons due to reduced GAM [29].

#159492 - $15.00 USD Received 7 Dec 2011; revised 3 Jan 2012; accepted 15 Jan 2012; published 23 Jan 2012

3.2. *Noise measurements*

The noise in the SC process can be divided into two contributions: a low-frequency part originating from technical laser noise and a broadband frequency part originating from amplified quantum noise [17, 30]. We will here concentrate on the broadband frequency part. RIN is quantified by the noise power in a 1 Hz bandwidth normalized to the DC signal power, $RIN = (\Delta P)^2/P_{avg}^2$, where $(\Delta P)^2$ is the mean square intensity fluctuation spectral density and P_{avg} is the average optical power.

The SC noise in Fig. 1(b) is characterized by white noise in between dc and the pump frequency, which was observed for all measured SCs. Thus, the RIN is dependent on the wavelength and input power, but to a good approximation independent of the electrical frequency.

Figure 3 shows the RIN as a function of SC wavelength and average input power for the uniform and tapered fiber, respectively. The thick black line indicates the spectral edges of the

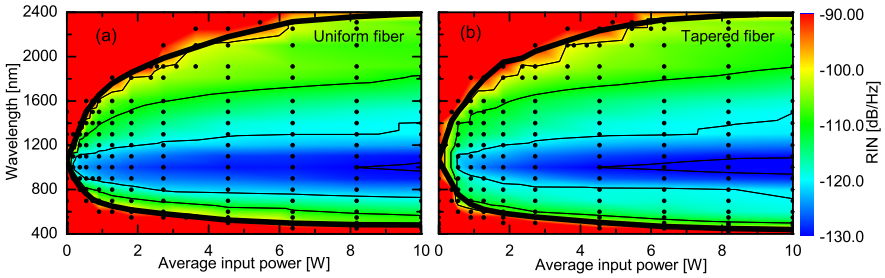

Fig. 3. RIN vs. input power and wavelength in (a) the uniform fiber and (b) the tapered fiber. The thick black line shows the spectral edges. The dots show the measurement points.

generated SC, defined at the -10 dBm/nm level, and the black dots indicate the actual measurement points, where the average RIN in the frequency region of 1-79 MHz has been measured. The noise properties of the SC generated in the two fibers are similar. At the spectral edge of the SC the RIN is about -100 dB/Hz. Generally, it decreases when the input power is increased (moving horizontally in Fig. 3) or the wavelength is chosen closer to the pump wavelength (moving vertically in Fig. 3). Thus, the minimum noise level of about -130 dB/Hz is observed close to the pump at a wavelength between 1000-1100 nm at the maximum input power level of 10 W. On the outer sides of the spectral edges the noise increases rapidly.

In Fig. 4(a) the RIN as a function of wavelength is compared for the uniform and the tapered fiber at two different power levels. The RIN of the tapered fiber is shown to be lower than the

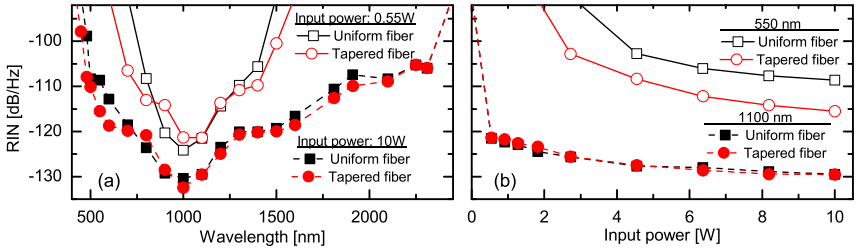

Fig. 4. RIN of the uniform (black squares) and the tapered fiber (red circles) (a) vs. wavelength at fixed input power of 0.55 W (open symbols) and 10 W (solid symbols) and (b) vs. input power at fixed wavelength of 550 nm (open symbols) and 1100 nm (solid symbols).

RIN of the uniform fiber for near-edge wavelengths. This is in good agreement with Kudlinski

#159492 - $15.00 USD Received 7 Dec 2011; revised 3 Jan 2012; accepted 15 Jan 2012; published 23 Jan 2012

et al. who have recently investigated the noise properties of tapered PCFs in the visible region [14]. They observed that the noise was reduced at the blue wavelength edge when the fiber was tapered and attributed it to a presumed increase of the spectral power density beyond 1750 nm. This increase will lead to increased probability to encounter solitons at the long wavelength side of the SC. Since the dispersive waves at the blue edge is group velocity matched to these solitons, the noise will also decrease in the blue edge of the SC. Our experiments show that for a *fixed* wavelength near the spectral edge the noise will decrease when the fiber is tapered. This is, however, only due to the fact that the spectrum generated in a tapered fiber is broadened. Thus, looking at a near-edge wavelength *relative* to the spectral edge, e.g. 20 nm from the edge, of a SC generated in a uniform and a tapered fiber, respectively, will yield the same noise level.

Figure 4(b) shows the RIN as a function of input power for the uniform and the tapered fiber at a near-edge wavelength and at a central wavelength. It is clearly seen that the noise properties at a central wavelength for the two fibers are close to identical while the tapered fiber exhibit lower RIN for a fixed near-edge wavelength, which again is in good agreement with [14].

To further quantify the noise on the spectral edges of the SCs we have measured the RIN by adjusting the input power so that the spectral edge at a level of -10 dBm/nm is equivalent to the central wavelength of the narrow band filters. The RIN in the 1600-2400 nm range was not measured due to less well-defined filters and a noisier photoreceiver. In Fig. 5 it is clearly seen

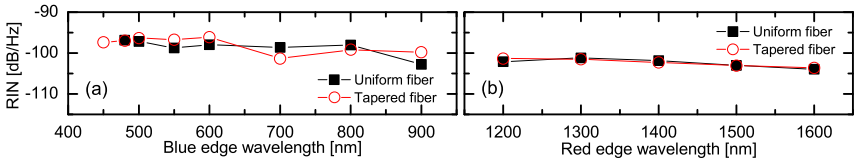

Fig. 5. RIN at the spectral (a) blue and (b) red edge of the uniform and tapered fiber, respectively, as a function of wavelength.

that the RIN level at the spectral edge is fixed at around -100 dB/Hz. The lower red edge noise level can be explained by the shape of the spectra. At the blue edge the spectrum is steep while it is more flat at the red edge. Since we have defined the edge to be at a level of -10 dBm/nm the the presence of a finite power spectral density (PSD) on the outer side of the red edge (below -10 dBm/nm) will lead to a reduction of the measured noise compared to the blue edge, where the is no PSD on the outer side of the blue edge because of the steep edge. Vanvincq *et al.* observed a significant reduction of power fluctuations at the long-wavelength edge of a SC generated in solid-core photonic bandgap fibers due to suppression of soliton self-frequency shift near the bandgap edge [19]. The dispersive waves below 550 nm in Fig. 5(a) will be matched to solitons above 2000 nm, i.e. solitons in the material loss region. Since we observe a nearly constant RIN in the blue edge, the materiel loss edge is thus not effecting the RIN.

4. Conclusion

We have experimentally investigated the RIN of picosecond SC generated at different power levels in uniform and tapered PCFs. When observing a fixed wavelength near the spectral edge the noise is reduced when the fiber is tapered. This reduction is however only due to the spectral shift of the spectrum. The noise at the spectral edge of a SC is constant independent of input power for both tapered and uniform fibers. An increase of power will generally lead to a decrease of noise for a fixed wavelength and the noise for a fixed power level will be lowest at the pump wavelength and highest at the spectral edges.

#159492 - $15.00 USD Received 7 Dec 2011; revised 3 Jan 2012; accepted 15 Jan 2012; published 23 Jan 2012

Acknowledgments

The authors acknowledge the H.C. Ørsted Foundation, Taumoses Legat, and the Danish Agency for Science, Technology and Innovation for the financial support of project no. 09-070566.

#159492 - $15.00 USD Received 7 Dec 2011; revised 3 Jan 2012; accepted 15 Jan 2012; published 23 Jan 2012